THE JOURNAL OF PHYSICAL CHEMISTRY B

Article

pubs.acs.org/JPCB

Calculations of Critical Micelle Concentration by Dissipative Particle Dynamics Simulations: The Role of Chain Rigidity

Ming-Tsung Lee, Aleksey Vishnyakov, and Alexander V. Neimark*

Department of Chemical Engineering, Rutgers, The State University of New Jersey, 98 Brett Road, Piscataway, New Jersey 08854, United States

Supporting Information

ABSTRACT: Micelle formation in surfactant solutions is a self-assembly process governed by complex interplay of solvent-mediated interactions between hydrophilic and hydrophobic groups, which are commonly called heads and tails. However, the head–tail repulsion is not the only factor affecting the micelle formation. For the first time, we present a systematic study of the effect of chain rigidity on critical micelle concentration and micelle size, which is performed with the dissipative particle dynamics simulation method. Rigidity of the coarse-grained surfactant molecule was controlled by the harmonic bonds set between the second-neighbor beads. Compared to flexible molecules with the nearest-neighbor bonds being the only type of bonded interactions, rigid molecules exhibited a lower critical micelle concentration and formed larger and better-defined micelles. By varying the strength of head–tail repulsion and the chain rigidity, we constructed two-dimensional diagrams presenting how the critical micelle concentration and aggregation number depend on these parameters. We found that the solutions of flexible and rigid molecules that exhibited approximately the same critical micelle concentration could differ substantially in the micelle size and shape depending on the chain rigidity. With the increase of surfactant concentration, primary micelles of more rigid molecules were found less keen to agglomeration and formation of nonspherical aggregates characteristic of flexible molecules.

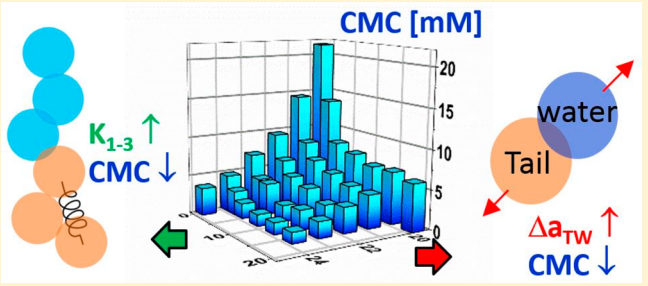

INTRODUCTION

Molecular architecture of surfactants determines the specifics of micelle formation and self-assembly in complex fluids. Once the concentration of surfactant exceeds the critical micelle concentration (cmc), the surfactant molecules aggregate into micelles, which differ in size and shape and coalesce further as the surfactant concentration increases. Theoretical prediction of cmc and micelle aggregation number (N_{ag}, the average number of surfactant molecules per micelle) for surfactants of given molecular structure has many important practical implications in colloid science and engineering. Micelle formation is governed by a complex interplay of solvent-mediated interactions between hydrophilic and hydrophobic groups, which are commonly called heads and tails. From the early 90s, micellization has been extensively studied using molecular simulations of surfactants modeled as head–tail chains of different architecture with the primary focus given to the head–tail repulsion and chain geometries.[1−4]

Another important factor determining micelle size and shape is the rigidity of surfactant molecule.[5] Although the importance of rigidity is well recognized, its impact on micellization has not been studied systematically. Several studies explore the effect of chain rigidity on micelle shape. Based on the experimental observations, Heerklotz et al.[6] hypothesized that a spherical micelle must contain very few highly ordered/stretched surfactant chains to shape the micelle and also a considerable number of highly disordered chains to fill its hydrophobic core. Increased rigidity of the tail segment may favor the formation of rodlike micelles. Sterpone et al.[7] studied the correlation of interfacial packing of alkyl-poly(ethylene glycol) type surfactants with different flexibility of surfactant hydrophilic head segment using molecular dynamics simulations. They found that "hydrophilic head acts as an entropic reservoir for overcompensating the positive enthalpic variation at sphere-to-rod transition". Thus, increased flexibility of the head segment may favor rodlike micelles, similarly to the effect of increased rigidity of the tail segment. Srinivasan and Blankschtein[8] looked into the role of rigidity in micellization by comparing the behavior of similar surfactants with alkyl and perfluoroalkyl tails. Fluorocarbons are effectively stiffer than hydrocarbons of similar molecular volume. The authors observed that increased rigidity caused fluorinated surfactants to form micelles of smaller curvature (that is, wormlike or bilayer) under the solution conditions, at which nonfluorinated surfactants would form spherical aggregates. Similar discussion about the rigidity affecting the micelle shape for perfluoroalkyl sulfonamide ethoxylate $C_8F_{17}EO_{10}$ can be found in ref 9. Firetto el al.[10] used grand canonical Monte Carlo simulations to study

Received: April 28, 2013
Revised: June 27, 2013
Published: July 9, 2013

   dx.doi.org/10.1021/jp4042028 | J. Phys. Chem. B 2013, 117, 10304−10310

the effect of chain rigidity on cmc and micelle size for the model surfactant composed of four head and tail groups, by changing the rigidity of the whole chain, and selectively of either hydrophobic or hydrophilc segment. Cmc was found to decrease and N_{ag} to increase with the chain rigidity, which is consistent with the experimental observation on fluorinated surfactants.[8] In a recent paper, Lin et al.[11] studied self-assembly of various model polymeric surfactants using dissipative particle dynamics (DPD) simulations and observed a decline in cmc with the greater degree of the rigidity of the solvophobic or solvophilic blocks. N_{ag} grew with the rigidity, but the shape of micelles remained approximately spherical. Wormlike micelles were observed in the concentrated solutions of rigid surfactants.

Recently, we showed[12] that DPD with rigorously defined soft-core repulsion interaction and rigidity parameters is capable of quantitative description of amphiphilic self-assembly in aqueous solutions. In DPD, molecules are modeled by soft quasiparticles (beads) connected by bonds. The parameters of soft potentials are fitted to thermodynamic[13,14] and/or structural[15−17] properties of the compounds of interest. In common DPD simulations of amphiphiles, bonded potentials are restricted to interactions between the nearest neighbors only ("1−2 interactions"). Such a simplification effectively neglects the rigidity of a molecule and is justified for coarse-grained models of polymeric chains with the bead size comparable to the persistence length. In fact, when DPD parameters are calculated[13] from the parameters of the Flory−Huggins model,[18,19] this assumption is implied. In practice, DPD is often applied to relatively small molecules (or large molecules whose composure require modeling with smaller beads[20,21]), and each bead of the model effectively represents a few actual atoms. The bead chain rigidity cannot be easily neglected in such systems, and this is recognized in the literature.[11,17,22] For example, Shillcock and Lipowsky[17] applied the chain rigidity to maintain stable lipid bilayer alignment. Ortiz et al.[22] fitted the parameters responsible for chain rigidity to end-to-end distances of polymer fragments obtained by atomistic MD simulations. Lin et al.[11] implemented rigidity in their DPD model by using a harmonic angle potential applied to two neighboring bonds in the polymer chain that is a standard approach in coarse-grained MD simulations.[10,23] In our recent paper,[12] chain rigidity was controlled by harmonic bonds between the second neighbors ("1−3 interactions") with bond rigidity inversely proportional to the number flexible torsions in the fragment of actual molecule represented by particular beads. We obtained quantitative agreement with the experimental cmc and aggregation number for several typical surfactants of different chemical structures.

In this paper, we examine the effect of molecule rigidity on the self-assembly of linear nonionic surfactants using conventional DPD simulations with the standard soft-core repulsion potentials. Chain rigidity is controlled using the second-neighbor (1−3) harmonic bonds.[12] Several simulations with the angle potential are performed for comparison. We focus on quantitative characterization of the most basic properties of dilute surfactant solutions: cmc, N_{ag}, and micelle shape.

SYSTEMS AND SIMULATION DETAILS

We consider two surfactants from our previous study:[12] octaethylene glycol monooctyl ether (C_8E_8) and *n*-decanoyl-*N*-methyl-D-glucamide (MEGA-10). Both molecules are relatively small, with molecular weights of 350 and 482 g/mol, respectively, and were modeled as linear chains of six (C_8E_8) and five (MEGA-10) soft beads connected by standard harmonic nearest-neighbor bonds. Thus, each bead represented only four −five heavy atoms and was substantially smaller than the persistence length. The coarse-grained models of the surfactant molecules and repulsive parameters are presented in Figure 1 and Table 1. The surfactants were dissected into tail T, head H, and middle M beads of the same size as the water bead W that represented $n_W = 4$ water molecules.

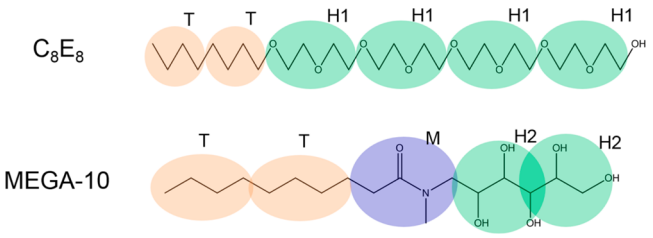

Figure 1. Schematic of coarse-grained surfactant models. C_8E_8 (octaethylene glycol monooctyl ether *n*-$C_8H_{17}(OCH_2CH_2)_8OH$) is presented as the chain of two tail and four head beads, TT-H1H1H1H1. MEGA-10 (*n*-decanoyl-*N*-methylglucamine, *n*-$C_9H_{19}(NCH_3)(HCOH)_4CH_2OH$) is modeled as a linear chain of two tail beads, one middle bead, and two head beads, TT-M-H2H2).

Table 1. Coarse-Grained Model of Molecules, Reference Compounds, and DPD Repulsive Parameters[a]

bead	reference compound	reference model	repulsive parameters k_BT/R_c
W	4 H_2O	W, monomer	$a_{WW} = a_{II} = 106.5$
T	$CH_3(CH_2)_6CH_3$	TT, dimer	$\Delta a_{TW} = 19.6$
M	$CH_3CON(CH_3)_2$	M, monomer	$\Delta a_{MW} = \Delta a_{MH2} = 3.0$, $\Delta a_{MT} = 3.0$
H_1	$CH_3OCH_2CH_2OCH_3$	H_1H_1, dimer	$\Delta a_{H1W} = 1.0$, $\Delta a_{H1T} = 6.5$
H_2	$OHCH_2(CHOH)_3CH_2OH$	H_2H_2, dimer	$\Delta a_{H2W} = 1.0$, $\Delta a_{H2T} = 9.8$

potential	definition of rigidity	K_{1-2}, K_{1-3}, K_θ	equilibrium length/angle
1−2 bond	$E = K_{1-2}(r_{i,i+1} - r_e)^2$	40 $[k_BT/R_c^2]$	0.8 $[R_c]$
1−3 bond	$E = K_{1-3}(r_{i,i+2} - r_e)^2$	0−20 $[k_BT/R_c^2]$	1.6 $[R_c]$
angle	$E = K_\theta(\theta - \theta_e)^2$	5−120 $[k_BT/\text{rad}^2]$	π

[a]Hydrophobic mismatch parameter is defined as $\Delta a_{IJ} = a_{IJ}a_{II}$.

In DPD, the system dynamics and equilibration are monitored by solving the equations of motion for the beads, which interact through pairwise conservative, drag, and random forces. Random $\mathbf{F}^{(R)}_{ij}$ and drag $\mathbf{F}^{(D)}_{ij}$ forces take into account fluctuation and dissipation of energy and serve as the Langevin thermostat. Conservative force $\mathbf{F}^{(C)}_{ij}$ accounts for nonbonded interactions; it is represented conventionally as a short-range harmonic repulsion

$$F^{(C)}_{ij} = a_{IJ}(1 - r_{ij}/R_c)(\mathbf{r}_{ij}/r_{ij}) \quad \text{at} \quad r_{ij} \le R_c,$$
$$F^{(C)}_{ij} = 0 \quad \text{at} \quad r_{ij} > R_c$$

where R_c is the effective bead diameter. The repulsion parameter a_{IJ} depends on bead types I and J to which beads i and j belong. We used the most common formulation of the method: the reduced density ρ^* of DPD beads (the average number of bead centers in 1 R_c^3) was set to $\rho^* = 3$, all beads

dx.doi.org/10.1021/jp4042028 | J. Phys. Chem. B 2013, 117, 10304−10310

had the same effective diameter R_c = 7.1 Å, and the self-repulsion parameter a_{II} was equal to $a_{WW} = 106.5k_BT/R_c$ for all bead types, as determined from the water compressibility as in ref 24. Conservative repulsion parameters between beads that belong to different types were determined from best fit to the infinite dilution activity coefficients of binary solutions formed by reference compounds that represent coarse-grained fragments of surfactant molecules, as described in ref 12. Parameter γ that determines the level of energy fluctuation and dissipation governed by random and drag forces was set to 1.5. Note that dynamic properties of micellar systems are not targeted in this work.

Table 1 lists the equations and parameters that define surfactant rigidity. Neighboring beads are connected by harmonic bonds, the choice of equilibrium bond length, and bond stiffness as described in ref 12. The rigidity of the coarse-grained surfactant molecule was controlled by imposing either the harmonic potential between the second-neighbor beads or the harmonic angle potential between the nearest-neighbor bonds, Figure 2. In the first method, each pair of beads that has

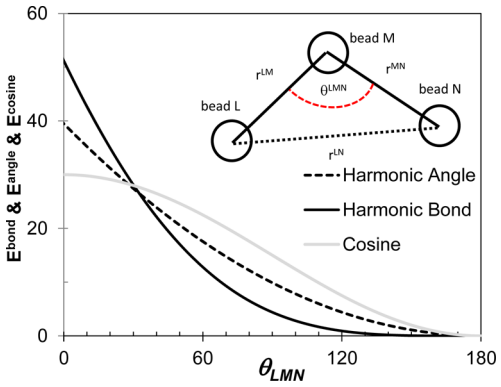

Figure 2. Two methods for accounting for the chain rigidity: second-neighbor (1−3) bond harmonic potential (solid line) and harmonic angle potential (dashed line). Cosine rigidity potential $E(\theta) = K_\theta(1 + \cos\theta)$ employed in previously published studies[10] is shown by gray line for comparison.

a common neighbor was connected by a "second-neighbor" harmonic bond whose equilibrium length was equal to the sum of the equilibrium lengths of the bonds to the common neighbor. For example, for a sequence of beads L−M−N, $r_e^{(LN)} = r_e^{(MN)} + r_e^{(LM)}$, $E^{LN} = K_{1-3}(r^{(LN)} - r_e^{(LN)})^2$. In the second method, the neighboring bonds were bound by a harmonic angle potential $E^{LMN} = K(\theta^{LMN} - \theta_e^{LMN})^2$. In both cases, the straight conformation corresponds to the minimum of potential energy. Compared to both harmonic[11] and cosine[10] angle rigidity potential, the second-neighbor bond potential is less stiff when $\theta \cong \pi$ but imposes a higher penalty at low angles ($\theta \cong 0$) (Figure 2). Although the harmonic angle potential is more conventional, we have to note that the rigidity potentials of coarse-grained molecules reflect torsional flexibility and 1−3 bonds may describe this flexibility more accurately than harmonic angles and cosine formula. Noteworthy, with such introduced second-neighbor 1−3 bond potentials, we obtained[12] quantitative agreement with the experimental cmc and N_{ag} for C_8E_8 and MEGA-10 (at $K_{1-3} = 20\ k_BT/R_c^2$) surfactants considered in this work.

Using the models and techniques described above, we calculated cmc and N_{ag} in model C_8E_8 and MEGA-10 surfactants for a wide range of hydrophobic mismatch Δa_{TW} and second-neighbor rigidity K_{1-3} parameters. The nearest-neighbor bonds had the same length and rigidity in all systems (Table 1). The list of systems modeled and average properties obtained is given in the Supporting Information, Table S1. We considered 65 micellar solutions with surfactant volumetric fraction ϕ ranging from 0.02 to 0.06. This concentration range lies below the critical aggregation concentration for the systems considered. Simulation length was 2×10^6 DPD steps; time step of $\tau = 0.02\tau$ (3.83 ps) was chosen to keep temperature deviation under 1%. The LAMMPS simulation package[25] was employed to perform DPD simulation.

Most simulations were performed in a cubic box of 30 × 30 × 30 R_c^3. Several additional simulations were performed in a larger box of 60 × 60 × 60 R_c^3 to confirm that the chosen box size of $30R_c$ provides sufficiently accurate results for both cmc and N_{ag} with relatively inexpensive simulations. The influences of the box size on the system equilibration and on cmc and N_{ag} with example of C8E8 solutions are described in the Supporting Information, section S−I. In order to evaluate the influence the of surfactant concentration on micellization, we performed simulations of MEGA-10 solutions at ϕ = 0.01−0.08 (see Supporting Information, section S−II).

By quantifying the amount of micelles and free surfactants, we found that equilibrium was established after 5×10^5 steps. Once in 1000 steps, configurations were saved for analysis. Two surfactant molecules were assumed to belong to the same aggregate if any two of their tail or middle beads overlapped. If an aggregate contained more than a certain threshold n_{mic} of surfactant molecules, it was counted as a micelle. If a surfactant molecule belonged to a cluster containing less than n_{mono} surfactant molecules, it was assumed to belong to the aqueous solution of monomers in equilibrium with the micelles. The concentration of "monomeric" surfactant in water was treated as the cmc. Aggregation was considered as complete and equilibrium reached when the cmc and micelle numbers stabilized and became practically insensitive to the choice of n_{mono} and n_{mic} within reasonable limits. In the "production" calculations, we used n_{mic} = 50 and n_{mono} = 10. A detailed discussion of choosing n_{mono} and n_{mic} can be found in ref 12. For cmc, statistical error calculated from mean square deviation ranged from 9% to 18%, with the averaged relative error of 14%. The deviation for N_{ag} ranged from 9% to 42%, based on the system and parameters.

RESULTS AND DISCUSSION

A compendium of the simulation results for all 65 systems considered is given in Table S1 of the Supporting Information. As a typical example, we present in Figure 3 the two-dimensional diagram of the cmc dependence on Δa_{TW} and K_{1-3} for MEGA-10 surfactant. The results obtained for two volume fractions of 2% and 4% confirm the accuracy of our calculations. This diagram shows that the cmc monotonically decreases with the increase of the hydrophobic mismatch parameters rigidity, so that the same cmc may correspond to the different sets of these parameters. The respective diagram of the N_{ag} dependence on Δa_{TW} and K_{1-3} in given in the Supporting Information, Figure S4b.

Figure 4 shows snapshots of C_8E_8 and MEGA-10 surfactant solutions at ϕ = 4%. We keep repulsive parameters as well as the parameters for nearest-neighbor bonds constant and adjust the second-neighbor bond rigidity K_{1-3} from zero (no rigidity, Figure 4a) to $20k_BT/R_c^2$ (Figure 4b). When no second-neighbor force is applied (K_{1-3} = 0), segregation is visually

dx.doi.org/10.1021/jp4042028 | J. Phys. Chem. B 2013, 117, 10304−10310

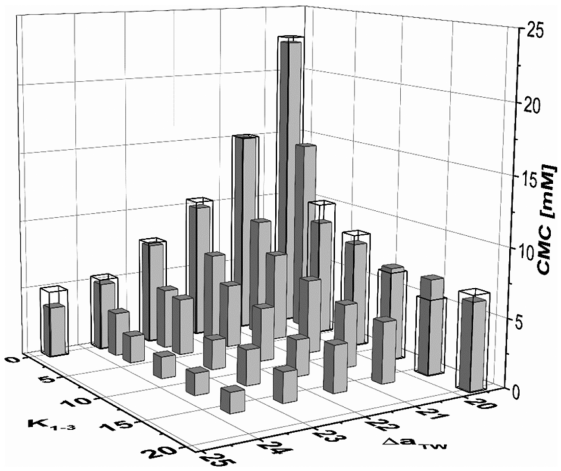

Figure 3. Dependence of the critical micelle concentration (cmc) on the second-neighbor bond rigidity (K_{1-3}) and hydrophobic mismatch (Δa_{TW}) parameters. MEGA-10 surfactant at volume fractions of 2% (open) and 4% (solid).

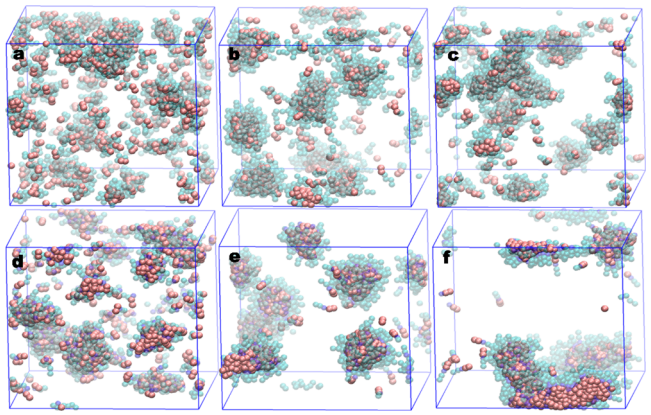

Figure 4. Micellization of C_8E_8 (a–c) and MEGA-10 (d–f) at 4% surfactant concentration. Head beads in cyan, tail beads in pink, middle beads in blue; water beads are not shown. (a) $\Delta a_{TW} = 19.6k_BT/R_c$, no chain rigidity is assigned, irregular segregation; (b) $\Delta a_{TW} = 19.6k_BT/R_c$, chain rigidity maintained by 1–3 bonds, $K_{1-3} = 20$, well-defined spherical micelles; (c) increased tail–water hydrophobic mismatch $\Delta a_{TW} = 23.6k_BT/R_c$, no rigidity with $K_{1-3} = 0$, agglomeration of micelles is evident. (d) $\Delta a_{TW} = 19.6k_BT/R_c$, no chain rigidity is assigned, irregular segregation; (e) $\Delta a_{TW} = 19.6k_BT/R_c$, modest stiff molecules with chain rigidity maintained by harmonic angles, $K_\theta = 5$, well-defined spherical micelles; (f) $\Delta a_{TW} = 19.6k_BT/R_c$, very stiff molecules with $K_\theta = 120$, wormlike micelles form.

evident but irregular (Figure 4a). The aggregate size distribution (Figure 5, dashed line) shows that the probability of finding a molecule in an aggregate of size N decreases nearly monotonically with N. It is not even clear that this system is indeed a micellar solution, since there is no clear qualitative criterion that allows distinguishing between "micelles" and smaller local "lumps," down to monomers dissolved in water.

The situation changes rapidly as the rigidity is introduced. With a modest rigidity of $K_{1-3} = 5k_BT/R_c^2$, the surfactant forms well-defined spherical micelles. The distribution of micelle sizes rapidly changes: a well-defined minimum separates micelles from short-living small aggregates that are normally observed in molecular solutions. The former can be characterized by size and shape, which we will describe later. The resulting cmc decreases steeply as K_{1-3} increases from 0 to $5k_BT/R_c^2$. A

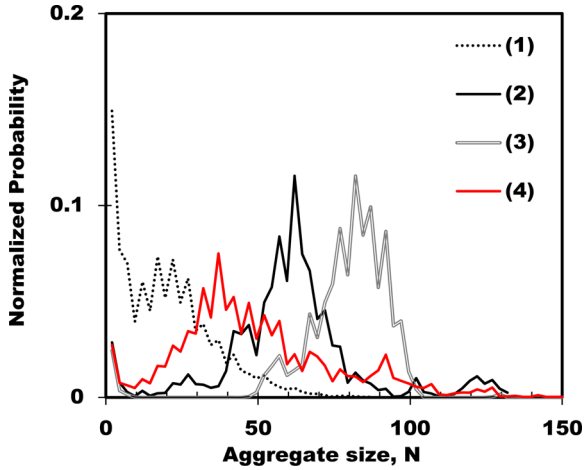

Figure 5. Probability distribution of finding a surfactant molecule in an aggregate consisting of N molecules for C_8E_8 at surfactant concentration of 4% vol. Line (1) (dotted): flexible model with no rigidity, $\Delta a_{TW} = 19.6k_BT/R_c$. Line (2) (black solid): $\Delta a_{TW} = 19.6k_BT/R_c$, rigidity applied using second-neighbor harmonic bonds, $K_{1-3} = 20k_BT/R_c^2$. Line (3) (hollowed): $\Delta a_{TW} = 19.6k_BT/R_c$, rigidity applied by harmonic angle potential, $K_\theta = 5k_BT/\text{rad}^2$. Line (4) (red solid): flexible chains with no rigidity with increased tail–water repulsion, $\Delta a_{TW} = 23.6k_BT/R_c$.

qualitatively similar observation was reported in ref 26 where aggregation of two-dimensional model surfactants was studies by off-lattice Monte Carlo. If K_{1-3} increases further, cmc appears to monotonically decrease as the surfactant molecule becomes more rigid. The micelles also become larger as K_{1-3} increases from 0 to $5k_BT/R_c^2$ as N_{ag} rises from 58 to 70, but further increase in rigidity hardly affects the micelle size, which remains constant within a statistical error. The general decline of cmc with rigidity agrees with the literature.[11,27]

Next, we examined whether the effect of rigidity could be effectively compensated by increasing the short-range conservative repulsion between surfactant tail beads and water beads. Figure 6a, b shows cmc and N_{ag} for MEGA-10 surfactant. MEGA-10 behaved qualitatively similar to C_8E_8 (Figure 6c, d). As the rigidity is introduced, cmc falls sharply and the micelle size increases. As K_{1-3} exceeds $5k_BT/R_c^2$, both properties show saturation with a modest influence of rigidity on cmc.

Figure 6 also shows cmc and N_{ag} for flexible (no second-neighbor bonds or angle potentials) surfactants with tails of different degrees of hydrophobicity quantified by the Δa_{TW} parameter (definition in Table 1). Naturally, Δa_{TW} significantly affects the cmc (Figure 6a, c, red circles), and strong hydrophobic tails make micellization well-defined (Figure 5). No "saturation" is observed in cmc vs Δa_{TW} dependence, which can be approximated as an exponential decay (shown in the Supporting Information, Figure S5a). cmc declines steeply as Δa_{TW} increases, similar to what we observed for cmc on increasing K_{1-3} and fixed Δa_{TW}. Thus, the effect of the rigidity on cmc can be easily mimicked via changing the short-range repulsion forces. For example, completely flexible MEGA-10 surfactant with $\Delta a_{TW} = 22.6k_BT/R_c$ has approximately the same cmc as a rigid surfactant with $\Delta a_{TW} = 19.6k_BT/R_c$ and $K_{1-3} = 16k_BT/R^2_c$.

The same, however, cannot be said about the micelle size and shape. For example, parts b and c of Figure 4 depict micellization of C_8E_8 in two systems with approximately the same cmc: in one system rigidity is produced by second-

dx.doi.org/10.1021/jp4042028 | J. Phys. Chem. B 2013, 117, 10304–10310

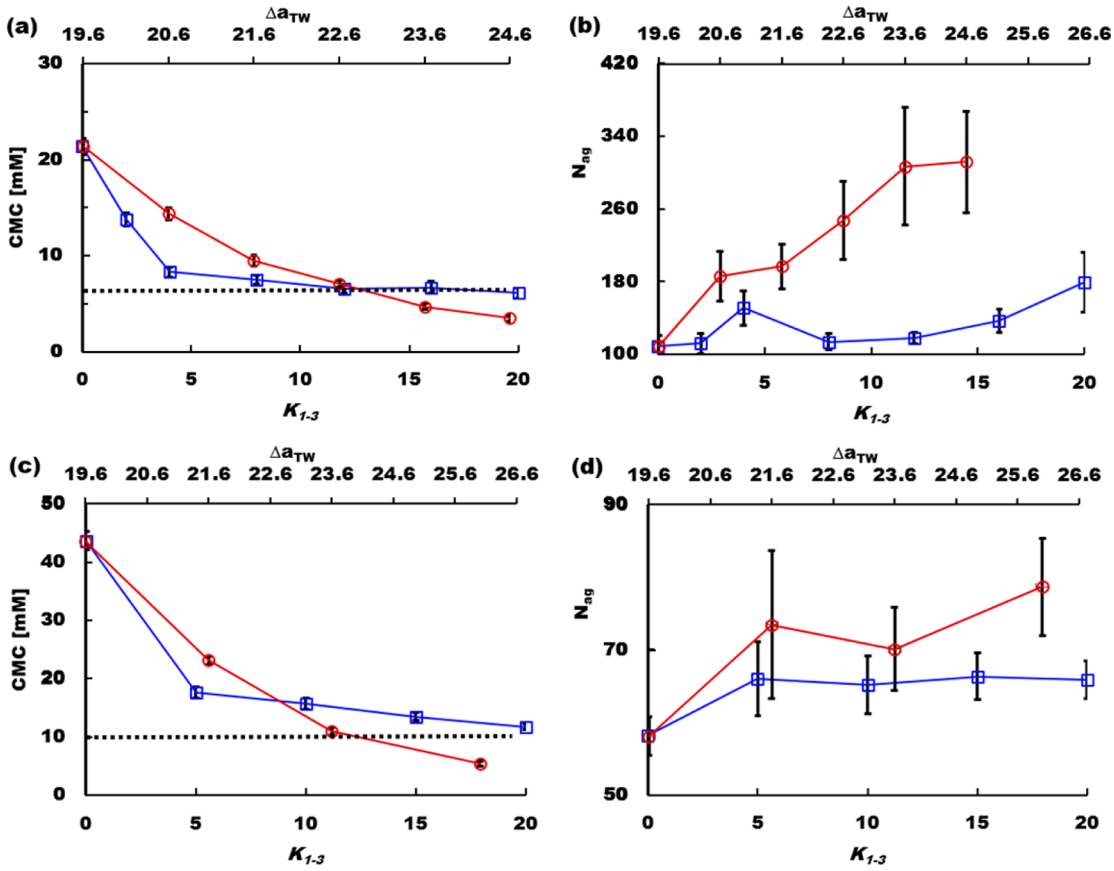

Figure 6. Averaged critical micelle concentration cmc and aggregation number N_{ag} of MEGA-10 (a, b) and C_8E_8 (c, d) at 4% surfactant concentration. Parameters (independent variables) are referred to the two abscissa axis: rigidity to the bottom axis (blue) and conservative mismatch Δa_{TW} to the upper axis (red). Ordinate show cmc (a, c) and N_{ag} (b, d) of the surfactants. Blue squares show the dependence of cmc and N_{ag} on K_{1-3} with a constant $\Delta a_{TW} = 19.6 k_B T/R_c$. Red circles show the dependence of cmc and N_{ag} on tail−solvent hydrophobic mismatch Δa_{TW} for flexible chains ($K_{1-3} = 0$). Black dotted lined indicate experimental cmc values for MEGA-10 (a) and C_8E_8 (c). Error bars for cmc are comparable with the symbol size.

neighbor bonds, and the other one formed by flexible molecules with Δa_{TW} increased from 19.6 to $\Delta a_{TW} = 23.6 k_B T/R_c$. The system formed by rigid molecules (Figure 4b) forms well-defined near-spherical micelles, while in the system of flexible surfactants with stronger tail−water repulsion, micelle aggregation becomes evident. Figure 6d shows that despite similar cmc, N_{ag} for the flexible system is greater approximately threefold.

The shape of the aggregated was quantitatively characterized by asphericity factor A,[28] a generalized quantitative measure of the departure from spherical symmetry for the gross shape of a polymeric molecule[29] or percolating clusters.[11] A is obtained from the gyration tensor **S** calculated for each micelle: $S_{ij} = (1/N)\sum_{l=1}^{N}(S_{il} - S_i^{CM})(S_{jl} - S_j^{CM})$ and S_i^{CM} stands for the center of mass in coordinate i (i denotes x, y, or z). After three eigenvalues R_1^2, R_2^2, R_3^2 of the gyration tensor are obtained, asphericity is calculated as $A = (1/(2R_g^4))[(R_1^2 - R_2^2) + (R_1^2 - R_3^2) + (R_3^2 - R_2^2)]$, where $R_g^2 = R_1^2 + R_2^2 + R_3^2$ is the radius of gyration. Asphericity ranges from 0 for spherically symmetric objects to 1 for an infinite cylinder. In Figure 7, we compare the distribution of asphericity for two C_8E_8 systems, which have the same cmc: rigid chains characterized by $\Delta a_{TW} = 19.6 k_B T/R_c$ and $K_{1-3} = 20 k_B T/R_c^2$ and flexible chains characterized by $\Delta a_{TW} = 23.6 k_B T/R_c$ and $K_{1-3} = 0$. In the latter case, the absence of rigidity is compensated by increased hydrophobic mismatch to provide the same cmc. Figure 7 clearly shows that the system with equal cmc values may exhibit drastically different patterns during the micellar self-assembly. The prominent peak at approximately $A = 0.09$ on the asphericity distribution corresponds to well-defined spherical micelles. In the flexible surfactant system, elongated nonspherical aggregates prevail. It appears from the snapshots shown in Figure 4c that the larger aggregates are formed by micelles merged by their hydrophobic cores instead of well-defined wormlike micelles that should precede the formation of hexagonal liquid crystal. We may assume that although the cmc values of these two model surfactants coincide, the critical aggregation concentrations, testing of which is beyond the capability of our simulations, should be drastically different.

In order to compare to what extend the choice of the rigidity potential affects the results of simulations, we studied micellization for very rigid surfactants, using the harmonic angle potential with K_θ ranging from 0 to 120 $k_B T/\text{rad}^2$. At relatively low K_θ values, the harmonic angle potential influences micellization similarly to the second-neighbor bond potential as shown in Figure 4d, e: the cmc decreases, while the micelle size increases, and micelles remain predominantly spherical (Figure 7). However, further increase in rigidity leads to the formation of large wormlike micelles. For example, the snapshot presented in Figure 4f shows both smaller spherical and larger wormlike micelles. In Figure 7, these two types of aggregates are evident from two peaks on the asphericity factor

dx.doi.org/10.1021/jp4042028 | J. Phys. Chem. B 2013, 117, 10304−10310

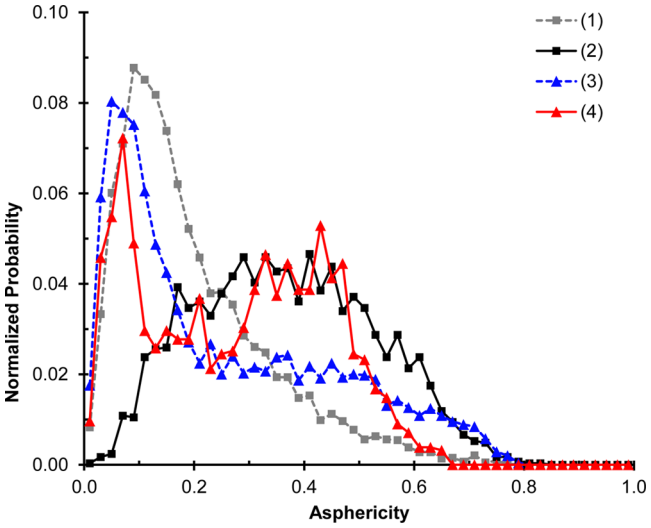

Figure 7. Distribution of the micelle asphericity factors in different systems. (1) Spherical micelles in C_8E_8 surfactant, $\Delta a_{TW} = 19.6k_BT/R_c$, rigidity applied using second-neighbor bond, $K_{1-3} = 20k_BT/R_c^2$. (2) Nonspherical symmetric aggregates in C_8E_8 type surfactant, flexible model with stronger tail−water hydrophobic mismatch, $\Delta a_{TW} = 23.6k_BT/R_c$, $K_{1-3} = 0$. (3) Mostly spherical micelles in MEGA-10 type surfactant, $\Delta a_{TW} = 19.6k_BT/R_c$, rigidity applied using the harmonic angle potential, $K_\theta = 5k_BT/\text{rad}^2$. (4) Wormlike micelles in MEGA-10 type surfactant, $\Delta a_{TW} = 19.6\ k_BT/R_c$, very rigid model, $K_\theta = 120k_BT/\text{rad}^2$.

distribution: a sharp peak around $A = 0.07$ corresponding to spherical micelles and a low broad peak ($A = 0.33-0.47$) corresponding to wormlike aggregates. We should note that such a stiff model can by no means represent MEGA-10; for example, a very rigid surfactant may be built with polyaromatic (such as rigid polyaromatic spacers are used in Gemini-type surfactants[30]), other polycyclic (such as sodium cholate[31]), or alkyne-type fragments. Because the rigid angle potential imposes constrains on conformations adopted by the tails, the tail beads cannot be efficiently packed inside the spherical micelle cores, which makes the spherical shape less favorable. Obviously, more efficient packing is possible within cylindrical micelle cores, which leads to the formation of wormlike micelles. Interestingly, cmc monotonically decreases with the rigidity, despite the disruption of the micelle core structure by the angle potential. The effect of rigidity is expected to be even stronger for longer amphiphiles such as block copolymers, where the packing of hydrophobic tails in micelle cores should be even more important than for short molecules studied here. Nevertheless, the effect of rigidity on the micelle shape is consistent with the experimental observations described in the Introduction.

CONCLUSION

In conclusion, the present work shows the importance of accurate accounting for the rigidity of molecules in DPD simulations of self-assembly processes, even in dilute surfactant solutions. We considered two common surfactants of different chemical structures: octaethylene glycol monooctyl ether and *n*-decanoyl-*N*-methylglucamine. Rigidity was introduced either with the second-neighbor harmonic bonds or harmonic angles potentials, so that the linear straight conformation corresponded to the minimum of intramolecular energy. We found that rigid surfactants had substantially lower cmc and form larger and better-defined micelles than flexible molecules with the same nonbonded interaction parameters. As rigidity increases further, its effect on micellization weakens significantly. The effects of rigidity on cmc and aggregation morphology are consistent to what were observed in the literature.[11] We also found that the effect of rigidity on cmc cannot be effectively mimicked by strengthening the hydrophobic mismatch between the hydrophobic tail and solvent beads: the parameters that produce the same cmc result in much higher average micelle size, as micelles of the more flexible surfactant easily aggregate and form larger agglomerates. Therefore, if we imagine a set of structurally similar linear surfactants with different tail hydrophobicity and chain rigidity but the same cmc, the aggregation number will have a minimum corresponding to the surfactants of intermediate rigidity: micelles formed by completely flexible surfactants tend to aggregate, while very rigid molecules tend to form well-defined rod-shaped micelles. As a methodological outcome, we conclude that the introduction of the second-neighbor harmonic bonds is a convenient and efficient method for accounting for the chain rigidity in DPD simulations. This potential can be parametrized from the analysis of the number of flexible angles in the coarse-grained chain fragment, as discussed in ref 12. The proposed method can be recommended for studies of self-assembly and dynamics in various soft matter systems beyond the surfactant solutions considered here.

ASSOCIATED CONTENT

Supporting Information

Section S−I includes the description of the additional simulations performed to analyze the influence of the box size (Figure S1) on the accuracy of cmc and N_{ag} calculation: we compare the micellization of C_8E_8 surfactant in $30 \times 30 \times 30$ R_c^3 and $60 \times 60 \times 60$ R_c^3 simulation boxes. We also demonstrate the dynamics of the equilibration process in DPD simulations of micellization. We conclude that the simulation box of $30R_c$ and the length of simulation runs used for "production" simulations are sufficient for providing quantitative results on cmc and N_{ag} with reasonable accuracy. Section S−II describes dependence of micelle structure and N_{ag} on surfactant volume fraction and explains the choice of concentration range and possible dependence of the apparent cmc on surfactant concentration. Figure S3 shows the asphericity factor distribution for MEGA-10 surfactant. Section S−III lists the parameters of the all 65 systems studied and the average properties obtained (Table S1). It also contains the alternative graphical presentations of cmc and N_{ag} for MEGA-10 model (Figures S4, S5). Section S−IV provides an alternative method for characterization of the micelle shape using the asymmetry factor. The asymmetry factor distributions given in Figure S6 are qualitative similar to those reported in Figure 7 for the asphericity factor. At the same time, the peaks on the asymmetry factor distributions are more pronounced (see Figure S6). This material is available free of charge via the Internet at http://pubs.acs.org.

AUTHOR INFORMATION

Corresponding Author

*E-mail: aneimark@rutgers.edu.

Notes

The authors declare no competing financial interest.

■ ACKNOWLEDGMENTS

This work was supported by the National Science Foundation, grant DMR-1207239.

■ REFERENCES

(1) Smit, B.; Esselink, K.; Hilbers, P. A. J.; Vanos, N. M.; Rupert, L. A. M.; Szleifer, I. Computer Simulations of Surfactant Self-Assembly. *Langmuir* **1993**, *9*, 9−11.
(2) Larson, R. G. Monte-Carlo Simulation of Microstructural Transitions in Surfactant Systems. *J. Chem. Phys.* **1992**, *96*, 7904−7918.
(3) Bernardes, A. T.; Henriques, V. B.; Bisch, P. M. Monte-Carlo Simulation of a Lattice Model for Micelle Formation. *J. Chem. Phys.* **1994**, *101*, 645−650.
(4) Cheong, D. W.; Panagiotopoulos, A. Z. Monte Carlo Simulations of Micellization in Model Ionic Surfactants: Application to Sodium Dodecyl Sulfate. *Langmuir* **2006**, *22*, 4076−4083.
(5) Marshall, B. D.; Emborsky, C.; Cox, K.; Chapman, W. G. Effect of Bond Rigidity and Molecular Structure on the Self-Assembly of Amphiphilic Molecules Using Second-Order Classical Density Functional Theory. *J. Phys. Chem. B* **2012**, *116*, 2730−2738.
(6) Heerklotz, H.; Tsamaloukas, A.; Kita-Tokarczyk, K.; Strunz, P.; Gutberlet, T. Structural, Volumetric, and Thermodynamic Characterization of a Micellar Sphere-to-Rod Transition. *J. Am. Chem. Soc.* **2004**, *126*, 16544−16552.
(7) Sterpone, F.; Briganti, G.; Pierleoni, C. Sphere Versus Cylinder: The Effect of Packing on the Structure of Nonionic C12e6b Micelles. *Langmuir* **2009**, *25*, 8960−8967.
(8) Srinivasan, V.; Blankschtein, D. Prediction of Conformational Characteristics and Micellar Solution Properties of Fluorocarbon Surfactants. *Langmuir* **2005**, *21*, 1647−1660.
(9) Sharma, S. C.; Abe, M.; Aramaki, K., Viscoelastic Wormlike Micelles in Nonionic Fluorinated Surfactant Systems. In *Self-Organized Surfactant Structures*; Tadros, T. F., Ed.; Wiley-VCH, Verlag GmbH & Co. KGaA: Weinheim, Germany, 2010.
(10) Firetto, V.; Floriano, M. A.; Panagiotopoulos, A. Z. Effect of Rigidity on the Micellization Behavior of Model H4t4 Surfactant Chains. *Langmuir* **2006**, *22*, 6514−6522.
(11) Lin, Y.-L.; Wu, M.-Z.; Sheng, Y.-J.; Tsao, H.-K. Effects of Molecular Architectures and Solvophobic Additives on the Aggregative Properties of Polymeric Surfactants, *J. Chem. Phys.*, **2012**, *136*.
(12) Vishnyakov, A.; Lee, M.-T.; Neimark, A. V. Prediction of the Critical Micelle Concentration of Nonionic Surfactants by Dissipative Particle Dynamics Simulations. *J.Phys. Chem. Lett.* **2013**, *4*, 797−802.
(13) Groot, R. D.; Warren, P. B. Dissipative Particle Dynamics: Bridging the Gap between Atomistic and Mesoscopic Simulation. *J. Chem. Phys.* **1997**, *107*, 4423−4435.
(14) Wijmans, C. M.; Smit, B.; Groot, R. D. Phase Behavior of Monomeric Mixtures and Polymer Solutions with Soft Interaction Potentials. *J. Chem. Phys.* **2001**, *114*, 7644−7654.
(15) Lebard, D. N.; Levine, B. G.; Mertmann, P.; Barr, S. A.; Jusufi, A.; Sanders, S.; Klein, M. L.; Panagiotopoulos, A. Z. Self-Assembly of Coarse-Grained Ionic Surfactants Accelerated by Graphics Processing Units. *Soft Matter* **2012**, *8*, 2385−2397.
(16) Lyubartsev, A. P.; Karttunen, M.; Vattulainen, I.; Laaksonen, A. On Coarse-Graining by the Inverse Monte Carlo Method: Dissipative Particle Dynamics Simulations Made to a Precise Tool in Soft Matter Modeling. *Soft Mater.* **2003**, *1*, 121−137.
(17) Shillcock, J. C.; Lipowsky, R. Equilibrium Structure and Lateral Stress Distribution of Amphiphilic Bilayers from Dissipative Particle Dynamics Simulations. *J. Chem. Phys.* **2002**, *117*, 5048−5061.
(18) Huggins, M. L. Solutions of Long Chain Compounds. *J. Chem. Phys.* **1941**, *9*, 440.
(19) Flory, P. J. Thermodynamics of High Polymer Solutions. *J. Chem. Phys.* **1942**, *10*, 51−61.
(20) Elliott, J. A.; Paddison, S. J. Modelling of Morphology and Proton Transport in Pfsa Membranes. *Phys. Chem. Chem. Phys.* **2007**, *9*, 2602−2618.
(21) Wang, Y. L.; Laaksonen, A.; Lu, Z. Y. Specific Binding Structures of Dendrimers on Lipid Bilayer Membranes. *Phys. Chem. Chem. Phys.* **2012**, *14*, 8348−8359.
(22) Ortiz, V.; Nielsen, S. O.; Discher, D. E.; Klein, M. L.; Lipowsky, R.; Shillcock, J. Dissipative Particle Dynamics Simulations of Polymersomes. *J. Phys. Chem. B* **2005**, *109*, 17708−17714.
(23) Marrink, S. J.; De Vries, A. H.; Mark, A. E. Coarse Grained Model for Semiquantitative Lipid Simulations. *J. Phys. Chem. B* **2004**, *108*, 750−760.
(24) Vishnyakov, A.; Talaga, D. S.; Neimark, A. V. DPD Simulation of Protein Conformations: From Alpha-Helices to Beta-Structures. *J. Phys. Chem. Lett.* **2012**, *3*, 3081−3087.
(25) Plimpton, S. Fast Parallel Algorithms for Short-Range Molecular Dynamics. *J. Comput. Phys.* **1995**, *117*, 1−19.
(26) Bhattacharya, A.; Mahanti, S. D.; Chakrabarti, A. Self-Assembly of Neutral and Ionic Surfactants: An Off-Lattice Monte Carlo Approach. *J. Chem. Phys.* **1998**, *108*, 10281−10293.
(27) Panagiotopoulos, A. Z.; Floriano, M. A.; Kumar, S. K. Micellization and Phase Separation of Diblock and Triblock Model Surfactants. *Langmuir* **2002**, *18*, 2940−2948.
(28) Rudnick, J.; Gaspari, G. The Asphericity of Random-Walks. *J. Phys. A: Math. Gen.* **1986**, *19*, L191−L193.
(29) Noguchi, H.; Yoshikawa, K. Morphological Variation in a Collapsed Single Homopolymer Chain. *J. Chem. Phys.* **1998**, *109*, 5070−5077.
(30) Zhang, Z.; Zheng, P.; Guo, Y.; Yang, Y.; Chen, Z.; Wang, X.; An, X.; Shen, W. The Effect of the Spacer Rigidity on the Aggregation Behavior of Two Ester-Containing Gemini Surfactants. *J. Colloid Interface Sci.* **2012**, *379*, 64−71.
(31) Sodium Cholate—Compound Summary (Cid 23668194); NIH: Bethseda, MD, 2010.